

# Photosensitization of CdSe/ZnS QDs and reliability of assays for reactive oxygen species production

Daniel R. Cooper,<sup>a</sup> Nada M. Dimitrijevic<sup>b</sup> and Jay L. Nadeau<sup>\*a</sup>

Received 16th June 2009, Accepted 24th August 2009

First published as an Advance Article on the web 29th September 2009

DOI: 10.1039/b9nr00130a

CdSe/ZnS quantum dots (QDs) conjugated to biomolecules that can act as electron donors are said to be “photosensitized”: that is, they are able to oxidize or reduce molecules whose redox potential lies inside their band edges, in particular molecular oxygen and water. This leads to the formation of reactive oxygen species (ROS) and phototoxicity. In this work, we quantify the generation of different forms of ROS from as-synthesized QDs in toluene; water-solubilized, unconjugated QDs; QDs conjugated to the neurotransmitter dopamine; and dopamine alone. Results of indirect fluorescent ROS assays, both in solution and inside cells, are compared with those of spin-trap electron paramagnetic resonance spectroscopy (EPR). The effect of these particles on the metabolism of mammalian cells is shown to be dependent upon light exposure and proportional to the amount of ROS generated.

## 1. Introduction

A photosensitizer (or photocatalyst) is any substance that upon absorption of light (ultraviolet, visible, or infrared) is able to transfer energy to another molecule; when the final acceptor molecule is water or oxygen, this leads to the generation of reactive oxygen species (ROS) which are lethal to bacteria, fungi, and mammalian cells. The use of photosensitizers to kill bacteria is highly effective and has been investigated since the middle of the nineteenth century, notably by Paul Ehrlich. The field was largely forgotten with the discovery of antibiotics, but has recently attracted increasing interest due to the emergence of antibiotic-resistant pathogens. Due to their high absorption and emission yields, most photosensitizers are organic dye molecules. Common bacterial strains such as methylene blue, acridine orange, and toluidine blue serve as non-specific bacterial stains as well as light-activated microbicides.<sup>1</sup> However, most dyes are photochemically unstable and may not be able to absorb light in the desired wavelength range. Since 99% of the energy output from the sun is in the visible range, it is desirable for photosensitizers for sunlight-mediated disinfection to absorb visible light. For medical applications, absorbance in the near-infrared range is desirable, as these wavelengths penetrate more deeply into tissues than visible light.<sup>2</sup>

The photocatalytic properties of semiconductor nanoparticles have been recognized for at least a decade as an important tool for environmental or therapeutic applications.<sup>3,4</sup> Nanoparticles are more photostable than dyes, the procedures for their synthesis are simpler, and their absorbance properties can be adjusted by varying particle material and size. TiO<sub>2</sub> and ZnS

particles have been made into solar cells; Ag and TiO<sub>2</sub> particles have been used as microbicides in anti-microbial clothing<sup>5</sup> and protocols for drinking-water purification.<sup>6</sup>

Fluorescent semiconductor quantum dots (QDs) have also been explored for these applications, although results in the literature have been contradictory. Some studies find significant ROS production from QDs, and others find none.<sup>7</sup> Cytotoxicity is often ascribed to “singlet oxygen” without a clear demonstration of the mechanism. Part of the problem is that QDs of different compositions (CdTe, CdSe, CdSe/ZnS) have been compared across studies when they each have very different photophysics. Another issue is that certain ROS reporter dyes may be directly oxidized by nanoparticles, thus leading to a positive signal even when no ROS is present. A recent study found that fluorescent reporters that created a signal when oxidized gave false-positive ROS results with fullerenes.<sup>8</sup> Only reporters that required reduction to generate the signal were reliable, notably the XTT assay. However, the same group found that despite their lack of ROS production, fullerenes were able to cause toxicity to bacterial cells by directly oxidizing membrane proteins.<sup>9</sup> Thus, observation of oxidative toxicity to cells does not necessarily imply ROS production.

Another issue is that there are many different mechanisms for ROS production and several different forms of ROS. Free radicals may be generated from photoexcited nanoparticles by either the *reductive pathway* (involving the electron transferring to an acceptor, A) or the *oxidative pathway* (involving the hole transferring to a donor, D) (Fig. 1A):



If the radicals formed interact with water or oxygen, ROS can result. However, the radicals might also recombine rapidly, such as in the “electron shuttling” seen with quinones,<sup>10</sup> for example by the process

<sup>a</sup>Department of Biomedical Engineering, McGill University, 3775 Rue University, Montreal, QC, H3A 2B4, Canada. E-mail: daniel.cooper@mail.mcgill.ca; jay.nadeau@mcgill.ca; Fax: +1 514 398 7461; Tel: +1 514 398 8372

<sup>b</sup>Center for Nanoscale Materials, Chemical Sciences and Engineering Division, Argonne National Laboratory, Argonne, IL 60439, USA

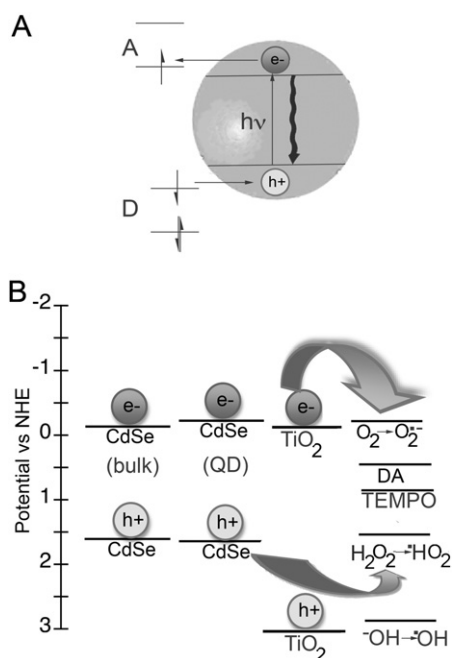
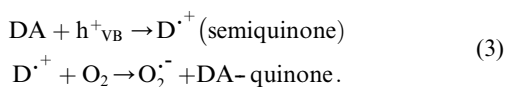


**Fig. 1** Mechanisms and energy levels involved in QD redox processes. (A) When a nanoparticle is excited by light more energetic than the band gap ( $h\nu$ ), an electron-hole pair (exciton) is formed. The electron may interact with an acceptor A, and/or the hole with a donor D. It is important to note that the electron wave function penetrates significantly into the surrounding solution whereas that of the hole does not. The donors must thus be strongly adsorbed to the nanoparticle for reaction to occur. (B) Approximate energy levels (vs. NHE) in aqueous solution for bulk CdSe (bandgap 1.7 eV) and a yellow CdSe QD (bandgap 2.1 eV as measured from absorbance peak).  $\text{TiO}_2$  is shown for comparison, as are the energies of the molecules appropriate to this study: dopamine (DA), TEMPO, oxygen, peroxide, and hydroxylate ions.



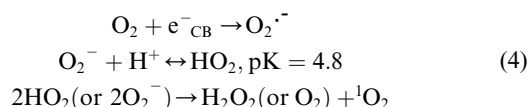
In this case, no ROS is produced and the presence of the radicals, which may have femtosecond lifetimes, is difficult to detect.

Can CdSe/ZnS QDs make ROS? The energy of a CdSe electron is very close to the redox potential of molecular oxygen (Fig 1B), making direct formation of large amounts of singlet oxygen unlikely. CdSe holes are highly oxidizing, but considerably less so than those of  $\text{TiO}_2$ , and might also be prevented from interacting by the ZnS shell. The formation of hydroxyl radicals directly is thus doubtful, but it could occur through an indirect mechanism, such as the photolysis of peroxide. In the presence of an electron-donating molecule such as dopamine (DA), however, the hole is expected to oxidize the DA, forming a semiquinone radical that can generate singlet oxygen:



The formation of singlet oxygen during autooxidation of dopamine and other catecholamines was reported earlier<sup>11</sup> and most probably involves semiquinone radicals, as fully chemically oxidized dopamine does not produce singlet oxygen.

At the same time, scavenging of holes by dopamine represses charge recombination, allowing for the increased yield of superoxide, and consequent formation of singlet oxygen:<sup>12</sup>



Thus, attachment of dopamine to QD (via conjugation of amino groups) can result in superoxide/singlet oxygen formation both in reduction and oxidation processes.

The goal of this work was three-fold. The first aim was to use spin-trap electron paramagnetic resonance (EPR) spectroscopy to distinguish between oxidative and reductive ROS production, and to compare these processes with QDs in organic solvent, water, and with dopamine conjugation. We found that QDs in toluene produced no substantial ROS. Solubilized, MPA-capped QDs produced oxidizing species but no significant singlet oxygen; the opposite was true of QD-dopamine.

The second aim was to compare and contrast these results with those obtained from fluorescent ROS reporters both in solution and in cultured mammalian cells, using several different types of reporter (sodium terephthalate, XTT, CM- $\text{H}_2\text{DCFDA}$ , and singlet oxygen sensor green). The tests in solution confirmed the EPR results and suggested that these reporter dyes do not show false-positive results with QDs. However, CM- $\text{H}_2\text{DCFDA}$  with cells was unreliable, possibly due to cap-decay of QDs outside cells which then interacted with the dye. Finally, we measured the metabolic effects of these conjugates on cells in order to determine the correlation between cellular ROS and metabolic inhibition. For this, we used the colorimetric 3-(4,5-dimethylthiazol)-2,5-diphenyltetrazolium bromide (MTT) assay. This assay is a standard measure of cell proliferation, and has been used in many studies involving QDs.<sup>13</sup> Here we found that a certain threshold concentration of QD-DA and a significant degree of light exposure were both necessary to observe metabolic inhibition in these cells. QDs alone showed very little toxicity, suggesting that the oxidative processes were not sufficient to cause cell death.

## 2. Materials and methods

### 2.1 QD synthesis and characterization

Chemicals were purchased from Sigma-Aldrich Canada (Oakville, ON). CdSe/ZnS QDs were synthesized using a method adapted from the literature<sup>14</sup> based on the noncoordinating solvent 1-octadecene (ODE). Briefly, 0.026 g of cadmium oxide (CdO) and 1 mL oleic acid (OA) were added to a three-necked flask containing 10 mL of ODE. This mixture was degassed and heated under  $\text{N}_2$  gas to 260 °C. The mixture turned colorless around 150 °C. The selenium (Se) precursor was prepared by mixing 0.01 g of elemental Se with 0.5 mL trioctylphosphine (TOP) under an inert atmosphere and sonicating until the solution became transparent. The zinc sulfide (ZnS) precursor was prepared as follows: 0.5 mL of TOP was combined with 0.2 mL hexamethyldisilathiane ( $(\text{TMS})_2\text{S}$ ) and 0.3 mL dimethylzinc ( $\text{Zn}(\text{CH}_3)_2$ ) under an inert atmosphere and diluted to 5 mL with ODE. Once the CdO/OA/ODE mixture reached 260 °C, the heat was turned off, and the Se precursor was injected rapidly using

a needled syringe. The ZnS precursor was injected over a time course of 5 min during the desired stage of QD growth. Afterwards, the temperature was allowed to drop to 100 °C and it was maintained at this temperature for several hours. The QDs were purified from the reaction side products by precipitation with acetone, anhydrous ethanol and chloroform, and resuspended in toluene. Mercaptopropionic acid (MPA) was used to replace the OA surfactant by a thiol-exchange reaction. 200 µL of concentrated QDs (optical density > 5) in toluene were added to 2 mL chloroform and 5 mL of methanol. 50 µL of MPA was added and the pH was adjusted to ~9–10 with tetramethylammonium hydroxide pentahydrate (TMAH). This solution was left at room temperature in the dark for 24 h. The thiol-modified QDs were separated from excess MPA ligand by precipitation and washing with ethyl acetate. The QDs were dried at room temperature under air and resuspended in distilled H<sub>2</sub>O (Millipore). Absorbance spectra were measured on a SpectraMax Plus plate reader, and emission spectra on a SpectraMax Gemini (Molecular Devices, Sunnyvale, CA).

## 2.2 Conjugation to dopamine

Dopamine hydrochloride (DA) was coupled to the QDs by a 1-ethyl-3-(3-dimethylaminopropyl)-carbodiimide hydrochloride (EDC)-mediated reaction. QDs in H<sub>2</sub>O were dialyzed (membrane cutoff 10 kDa) against PBS for 1 h and diluted to a final concentration of 1 µM. EDC and DA were added to the reaction mixture at a ratio of 1500 : 500 : 1 QD. The mixture was reacted for 30 min under gentle shaking and purified from excess side products by precipitation with THF and resuspension in PBS. The level of DA binding was quantified using the fluorescent indicator *o*-phthalaldehyde (OPA) as described.<sup>15</sup> For EPR studies, the conjugates were not purified or tested with OPA, but used immediately after preparation.

## 2.3 EPR spectroscopy

EPR spectra were collected on a Bruker Elexys E580 spectrometer at room temperature, with a power of 66.32 mW and a modulation amplitude of 1.0 Gauss. Illumination was with a 300 W Xe lamp (ILC Inc.) using a cutoff filter of 400 nm longpass, intensity ~100 mW cm<sup>-2</sup>. The changes in spin-trap concentration over time were determined by measuring EPR spectra at certain time intervals, while solutions were under continuous illumination. Typically, the accumulation of a single spectrum (sweep time) was 42 s in all experiments. The concentration of radicals was determined after double integration of spectra, and normalized to the 10 µM TEMPO radical. The *g* tensor values were calibrated for homogeneity and accuracy by comparing to a coal standard ( $g = 2.00285 \pm 0.00005$ ). The concentration of TMP was 0.1 M for all solutions; the concentration of TEMPO was varied, for conjugated QDs it was 33 µM. All solutions were in air. Some samples were bubbled with oxygen (and sealed), leading to a subsaturated solution of O<sub>2</sub>. Controls for QD–dopamine included DA alone and DA + EDC at the same concentrations as used for conjugation.

## 2.4 ROS assays in solution

All fluorescent assays were read in a 96-well black plate (Corning) in a Gemini EM plate reader (Molecular Devices).

Colorimetric assays were read in a clear 96-well plate on a SpectraMax UV–Vis spectrometer (Molecular Devices). For all assays, QD concentrations ranged from 0.1–1 µM. Duplicate samples were prepared for each condition, one to be blue light-exposed and the other aged under room oxygen but not light-exposed. The unexposed side of the plate was screened with aluminium foil. The lamp for exposure was a custom 96-LED lamp made of 2.5 mW, 440 nm LEDs arranged in the format of a 96-well plate to ensure uniform irradiation to each well. The generation of singlet oxygen was assayed using 1 µM singlet oxygen sensor green (SOSG) (Invitrogen) with excitation at 504 nm and emission at 514–600 nm. The generation of hydroxyl radicals was measured with sodium terephthalate following published methods.<sup>16</sup> Briefly, QDs were mixed with disodium terephthalate (1 mM) (Sigma Aldrich) and irradiated. Aliquots of the reaction mixture were withdrawn at 10 min time intervals, treated with 0.5 volumes of 1 M NaOH and monitored by fluorescence emission with excitation at 300 nm. The colorimetric formation of XTT formazan was used to measure HO<sub>2</sub>•/O<sub>2</sub>•<sup>-</sup> generation.<sup>17</sup> The generated radicals reduce the tetrazolium dye sodium-3'-(1-[phenylamino-carbonyl]-3,4-tetrazolium)-bis(4-methoxy-6-nitro) benzene-sulfonic acid hydrate (XTT) (Sigma Aldrich), which was added to the QDs at 1 mM. After the indicated period of irradiation, absorbance was measured at 470 nm.

## 2.5 Incubation of QDs with cells and ROS generation/MTT assay

Experiments with cell lines were performed using PC12 cells stably transfected with human D2 dopamine receptors (gift of Stuart Sealfon, Mount Sinai School of Medicine; selectable marker G418). Cells were maintained in high-glucose Dulbecco's Modified Eagle's Medium (DMEM) (Invitrogen Canada, Burlington, ON) supplemented with 10% fetal bovine serum, 5% horse serum, 0.2 mM glutamine, 100 U mL<sup>-1</sup> penicillin, 100 µg mL<sup>-1</sup> streptomycin and 500 µg mL<sup>-1</sup> G418 in a 5% CO<sub>2</sub> atmosphere at 37 °C. For passage, cells were rinsed first with phosphate-buffered saline (PBS) and then with Hank's balanced salt solution containing 0.05% trypsin and 0.02% EDTA, incubated for 2 min at room temperature, and resuspended in supplemented DMEM. Cells were passaged onto glass-bottom dishes (MatTek, Ashland, MA) or 96-well plates (Fisher Scientific) the day before use at 50–80% confluency. Just prior to labeling, growth medium was removed by two washes in sterile PBS, and then replaced with 1 mL serum-free medium without phenol red (OptiMem, Invitrogen). In preliminary studies, incubation times were varied between 15 min and 2 h, and it was found that some uptake of unconjugated QDs could occur at longer time scales. Thus, all data presented show cells incubated for 2 h unless stated otherwise, to permit possible identification of ROS generated in cells from unconjugated QDs. Unconjugated QDs or QD–dopamine conjugates were applied directly into serum-free medium at a concentration of ~5–10 nM particles. For co-labeling with LysoTracker Red or MitoTracker Orange (Invitrogen), dye was added to cells at a concentration of 1 µM at least 30 min before the end of the QD incubation. All cells were washed several times with sterile PBS after labeling and live cells were imaged in PBS.

ROS generation inside cells was quantified using 5-(and-6)-chloromethyl-2',7'-dichlorodihydrofluorescein diacetate, acetyl ester (CM-H<sub>2</sub>DCFDA) (Invitrogen). After incubation with QDs, cells were washed with PBS, and the medium replaced with PBS containing 10  $\mu$ M dye. After incubation for 30 min, cells were once again rinsed in PBS and the fluorescence spectrum taken with excitation at 485 nm. The wells were then irradiated in 10-min intervals using a hand-held UV lamp at wavelength of 365 nm for varying time periods (approximate emission power, 2.5 mW) (UVP, Upland, CA). Wells not to be irradiated were shielded with aluminium foil. Controls included cells with no dye; dye with no cells; cells with conjugate dopamine without QDs; and cells with dopamine with QDs but not conjugated.

The protocol for the MTT [3-(4,5-dimethylthiazol-2-yl)-2,5-diphenyltetrazolium bromide] colorimetric assay followed published methods.<sup>18</sup> PC12 cells were plated into 96-well plates at 50–80% confluency 1–2 days preceding the assay. Dopamine-CdSe/ZnS conjugates with varying concentrations were prepared in serum-free, phenol-red-free medium, and 200  $\mu$ L of the conjugates was added to each well and incubated for 30–60 min. After washing with PBS, 200  $\mu$ L PBS was added to each well and the wells were irradiated as described for the ROS assay. The PBS was then replaced with complete medium and the cells were further incubated for 18–24 h. 12.5  $\mu$ L of a 5 mg mL<sup>-1</sup> MTT solution in PBS was added to each well and incubated for 4 h. The resulting crystals were dissolved in dimethyl sulfoxide (200  $\mu$ L in each well) and absorbance measured at 570 nm.

For Hg-lamp exposure studies of single cells, cells were examined and imaged with an Olympus IX-71 inverted microscope and a Nuance multispectral imaging system, which provides spectral data from 420–720 nm in 10 nm steps (CRI Instruments, Cambridge, MA). The objective lens was a Nikon PlanFluor 100 $\times$  (N. A. = 1.30). Illumination was through a Quantum Dot filter cube set (excitation = 380–460 nm, dichroic = 475 nm, emission = 500 LP) or a DAPI filter cube set (excitation = 350/50 nm, dichroic = 400 nm, emission = 420 LP) (Chroma Technologies, Rockingham, VT). Confocal imaging was performed on a Zeiss 510 LSM with a PlanApo 1005 oil objective. QDs were excited with an Ar ion laser 488 nm line. LysoTracker Red and MitoTracker Orange were excited with a HeNe laser (543 nm line). Cells labeled with >1 probe were examined for channel bleed-through before imaging.

### 3. Results

#### 3.1 QD characterization

In this study we used yellow-emitting CdSe/ZnS QDs (QD590, emission peak 595  $\pm$  20 nm) for all experiments. This wavelength allowed for easy distinction from cellular autofluorescence, organelle dyes, and ROS indicators. Dopamine altered the optical properties of the particles, primarily by fluorescence quenching (Fig. 2A). The conjugation of dopamine molecules was confirmed by gel electrophoresis<sup>19</sup> (Fig. 2B) and quantified by spectroscopy. When bound by their primary amino group to functional groups on the QD surface, dopamine has neutral charge. Therefore, the effect of binding is a reduction in the net surface charge of the particles. In gel electrophoresis, QD–dopamine migrated towards the positive electrode at a slower

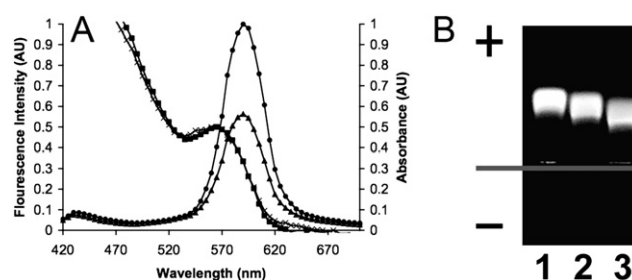


**Fig. 2** Optical and electrophoretic properties of QDs in this study. (A) Absorbance and normalized fluorescence intensity for QDs before and after conjugation to dopamine. The absorbance spectra are nearly identical between the QDs alone (■) and the conjugate (×). The emission spectra indicate partial quenching of the conjugate (▲) relative to the QDs alone (●). (B) Confirmation of conjugation reactions by gel electrophoresis. Lane 1: solubilized QDs alone; lane 2: QD–DA (ca. 62 ligands/particle) lane 3: QD–DA (ca. 140 ligands/particle). The sample corresponding to lane 3 was used for cell-labeling and toxicity experiments. The gray line indicates the sample loading position on the gel.

rate than the unmodified QD control indicating successful conjugation of these ligands. It was necessary to optimize the coupling reactions in order to modify only a portion of the surface. MPA-coated QDs are charge-stabilized and complete loss of charge resulted in particles that were unstable in solution. Not surprisingly, QDs saturated with dopamine remained in the loading well during gel electrophoresis, indicating macroscopic aggregation (not shown).

#### 3.2 EPR

The EPR spin-probe 2,2,6,6-tetramethyl-1-piperidinyloxy (TEMPO) is a stable free radical that can be oxidized by holes, OH radicals, or any other oxidative species that have a redox potential  $\geq$  +0.75 V vs. NHE (refer again to Fig. 1B). Thus the disappearance of TEMPO radical EPR spectra upon irradiation indicates photogenerated oxidative species. We found significant decay of TEMPO signals only upon illumination of QD–MPA, but not for QD–DA or QDs in toluene (Fig. 3A, B).

The TMP method measures the formation of singlet oxygen or superoxide anion using EPR-silent 2,2,6,6-tetramethylpiperidine (TMP). The reaction of non-paramagnetic species TMP with singlet oxygen/superoxide yields formation of a stable, EPR-sensitive radical adduct (nitroxide-type radical). In this case it is thus the formation of the radical rather than its disappearance which is measured, and the kinetics of formation can give a clue to the mechanisms. We found significant TMP-radical signals only with QD–DA, which increased when the solution was bubbled with oxygen (Fig. 3C, D).

#### 3.3 ROS assays

Singlet oxygen sensor green (SOSG) has been reported to be highly specific for <sup>1</sup>O<sub>2</sub>, and to respond very little to hydroxyl radicals or peroxide.<sup>16</sup> As in our previous work,<sup>20</sup> we found a significant signal from SOSG with QD–DA, but not with dopamine alone, QD–MPA, or the dye alone (Fig. 4A). Correspondingly, the hydroxyl radical sensor sodium terephthalate showed a signal only with QD–MPA (Fig. 4B).

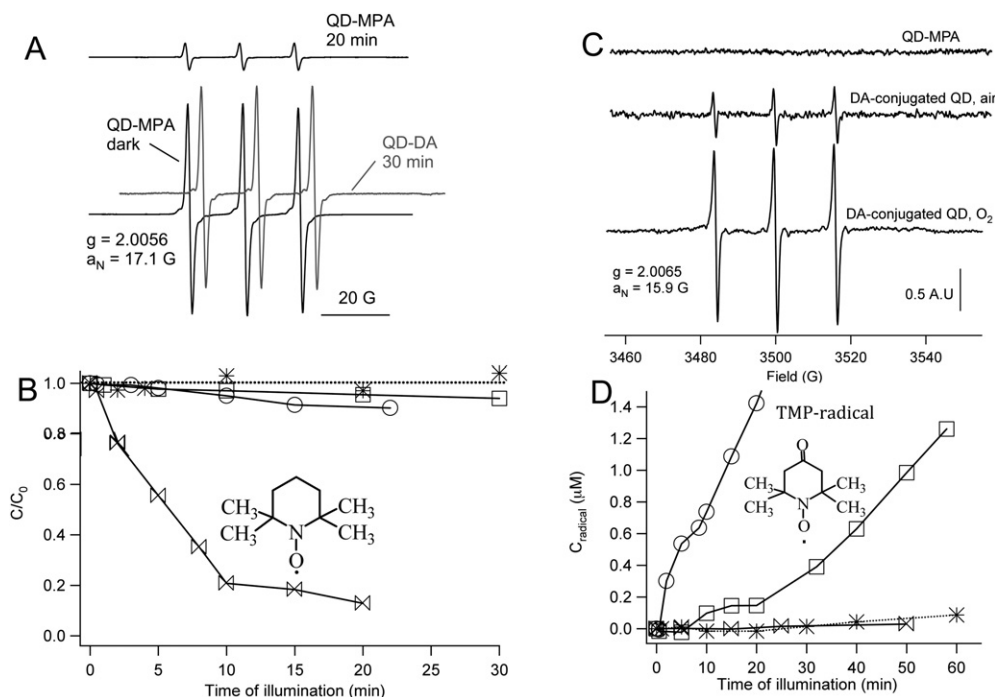


**Fig. 3** EPR spectroscopy using TMP and TEMPO radicals as spin traps. (A) the spectra of TEMPO radicals showing initial intensity of QD-MPA vs. substantial decay at 20 min. The QD-DA signal remained essentially constant with time (gray line, the spectrum is shifted for better visibility). (B) Decay of TEMPO radical relative concentrations with time of illumination showing QD-MPA (x), QD-DA (□), DA alone (\*), and hydrophobic QDs in toluene (○). Only QD-MPA shows a significant effect. (C) Spectra of TMP-radicals formed upon 60 min of illumination. The QD-MPA does not show any formation of TMP-radical, while QD-DA showed a significant effect, which increases with oxygen. (D) Concentration of formed TMP-radical vs. irradiation time for QD-MPA (\*), DA only (x), and QD-DA in air (□) vs. bubbled with oxygen (○).

XTT is unique in that it must be reduced, rather than oxidized, to yield a signal. Thus direct oxidation by the nanoparticles will not yield a false positive.<sup>8</sup> It is also more quantitative than the fluorimetric assays. XTT is sensitive to perhydroxyl and superoxide radicals, and thus might be expected to give a signal both with QD-MPA and QD-DA. This is indeed what we found, although the kinetics of the reactions differed. QDs alone showed a rapid increase in signal with a plateau after approximately 20 min of irradiation; QD-DA showed a more gradual increase throughout the irradiation period. With 100 nM QDs, the final amount of radical

produced was very similar after the 60 min period (6.6 μM for QD-DA vs. 6.4 μM for QD-MPA, using the published extinction coefficients<sup>21</sup>). However, with 200 nM QDs, the final values were 8.0 μM for QD-DA and 10.5 μM for QD-MPA (Fig. 4C).

### 3.4 Generation of ROS in D2-receptor bearing PC12 cells

QD-dopamine and unmodified QDs both showed substantial uptake by our dopamine-receptor-bearing PC12 cells after 30–120 min of exposure to 10 nM concentrations (Fig. 5A–C).

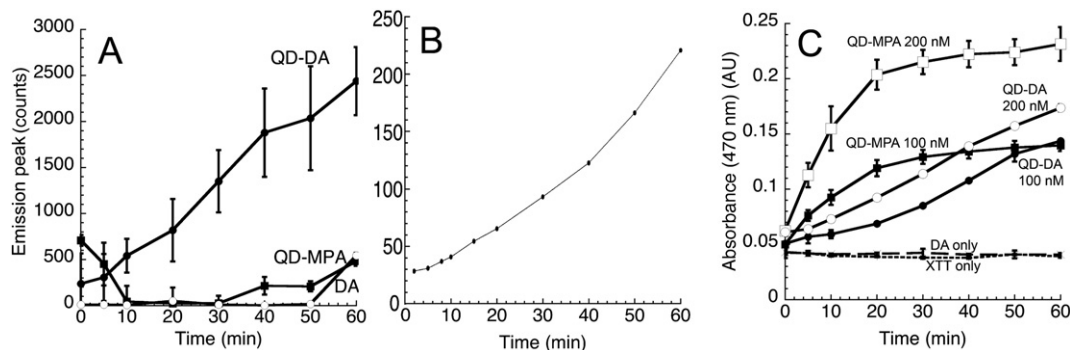


**Fig. 4** Fluorescent and colorimetric ROS assays in solution. Data points are averages of 3–5 experiments with error bars shown; when error bars do not appear, they are smaller than the symbols. (A) Singlet oxygen sensor green, peak at 530 nm. The signal from dye alone was subtracted. Shown are QD-DA and QD-MPA (at 100 nM), and DA alone (at 100 μM). (B) Sodium terephthalate peak at 435 nm from QD-MPA at 250 nM. (C) XTT. There was no signal from dye alone or DA alone. Two concentrations of QD-MPA and QD-DA are shown: 100 and 200 nM. Note the different kinetics with QD-MPA vs. QD-DA.

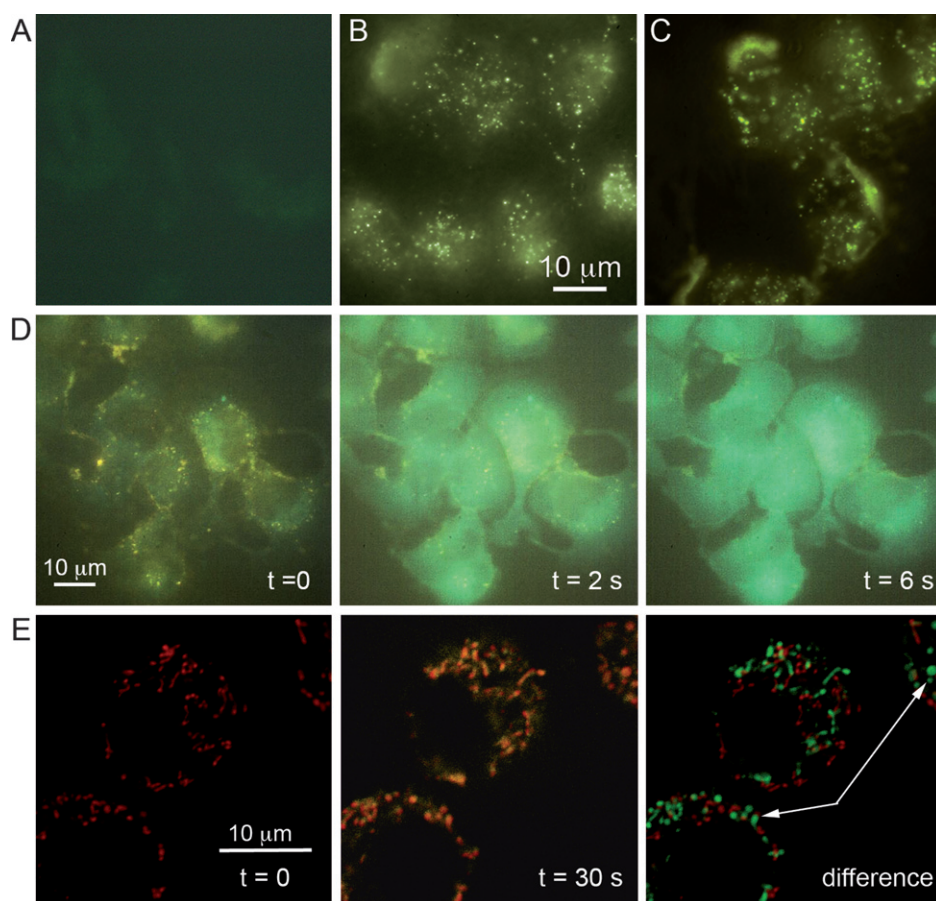


**Fig. 5** Uptake and processing of QDs and conjugates by PC12 cells. (A) PC12 cells alone under the QD filter (see Methods). (B) Unmodified QD-MPA, 5 nM exposed for 2 h, showing an endosomal uptake pattern. (C) QD-DA, 5 nM for 1 h, also showing intracellular vesicles consistent with endosomal uptake. (D) Photoenhancement of QD-DA under the DAPI filter. The photoenhancement of QD-DA has been studied in detail in ref. 22. Note the vesicular labeling that travels throughout the cell during the course of a few seconds of high-power Hg lamp exposure. (E) Photoenhancement and mitochondrial toxicity with QD-DA under confocal laser illumination. From  $t = 0$  to 30 s, a brightening of the QD fluorescence (yellow) is seen over the MitoTracker Dye (red). In the last panel, the QD fluorescence has been removed, and the difference in the MitoTracker signals from  $t = 0$  and 30 s is shown, with green indicating the later time point. Note the significant rounding of mitochondria (arrows).

One striking feature of QD-dopamine that we have previously reported is photoenhancement of internalized QDs, especially those associated with mitochondria.<sup>22</sup> Fluorescence in lysosomes faded rapidly, either due to the internal chemistry of these organelles or because light-induced rupture allowed lysosomal QDs to travel elsewhere in the cell (Fig. 5D). Labeling with specific dyes such as LysoTracker and Mitotracker enabled QD localization to these organelles to be identified and specific patterns to be identified. When QD-DA was present, mitochondrial-associated QD fluorescence increased with photoexposure, paralleling classic signs of mitochondrial toxicity such as rounding of the mitochondria within 30 s of confocal laser exposure (Fig. 5E).

In order to quantify intracellular ROS generation, we used CM-H<sub>2</sub>DCFDA, which measures generation of ROS inside cells only. It must be modified twice in order to become fluorescent: first deacetylated by intracellular esterases, then oxidized.<sup>23</sup> Thus, this assay should be a measure of relative QD uptake by the cells as well as of the capacity of the internalized QDs to generate ROS. When the dye was added after QD internalization, the results were sometimes consistent with ROS generation from

QD-DA conjugates but little from QD-MPA or DA alone (Fig. 6A). However, we found that the QDs alone sometimes interacted with the dye, generating large signals external to the cells that could be rinsed away. In this case the QDs alone gave greater signals than any of the conjugates (Fig. 6B). This occurred to different extents in different assays, perhaps reflecting the number of QDs that remained outside the cells when the dye was added. It had a poor correlation with concentration (note that the highest signal was seen with the lowest QD concentration used, 0.1 nM).

### 3.5 Effects on PC12 cell metabolism

Dopamine alone did not lead to any significant metabolic inhibition. Unconjugated QD-MPA showed a small (statistically insignificant) effect that was not measurably affected by irradiation. QD-dopamine was not significantly effective at concentrations below 10 nM or for irradiation times < 40 min. However, above these concentrations and exposure times, the effects on cells were marked, reducing metabolic activity to one-fifth of its original value (Fig. 7).

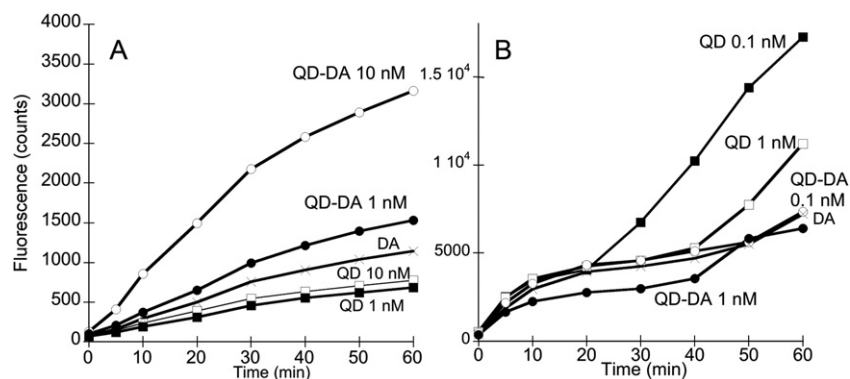


**Fig. 6** Variability of CM-H<sub>2</sub>DCFDA assay in PC12 cells exposed to QDs for 30–60 min and irradiated in 10-min increments. All values were consistent among triplicates done in the same experiment, with error bars smaller than symbols. (A) A “successful” assay. QD–DA shows a significant, time- and concentration-dependent signal. 100 μM dopamine alone shows a much smaller signal, and QD–MPA show a negligible signal. (B) An “erroneous” assay. Note the very different scale on the y-axis. Very large signals are seen with very low concentrations of QDs alone. Although QD–DA shows a signal comparable to that in (A), it is swamped by that of the QDs alone.

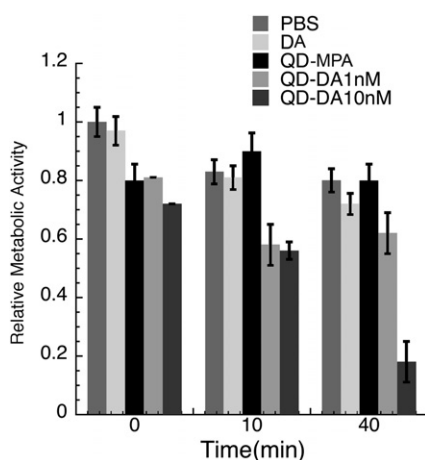


**Fig. 7** Effect of QDs and conjugates on cellular metabolism as measured by the MTT assay. All assays were performed 2–3 times on independent plates and error bars indicate the standard error of the mean. Controls consisted of cells with mock application of PBS and with DA alone (100 μM). Although QD–MPA had a significant effect on cells without irradiation ( $p < 0.05$ ), there was no significant difference between irradiated cells exposed to QDs or DA alone. A significant pattern of inhibition is not seen except in 10 nM QD–DA irradiated for 40 min or more ( $p < 0.001$ ).

#### 4. Discussion and conclusions

The phototoxicity of nanoparticles, particularly quantum dots, has been known for some time. However, while core CdSe<sup>24</sup> and CdTe<sup>13</sup> are extremely efficient at ROS generation, it has been suggested that core/shell CdSe/ZnS does not produce significant ROS by itself.<sup>7,20</sup> However, there is a large variation in shell thickness in different CdSe/ZnS preparations, and also a large difference in homemade vs. commercial QDs, both in shell synthesis methods and solubilization ligands. Recent reports also call into question the validity of fluorescent reporter assays for ROS when used with nanoparticles, since these reporter dyes might be directly oxidized, giving a false-positive signal.

In this work we show that CdSe/ZnS QDs, unlike C<sub>60</sub>, does indeed make reactive oxygen species, although negligible singlet

oxygen. Results of spin-trapped EPR and fluorescent and colorimetric reporter dyes are consistent. The MPA-capped QDs generate perhydroxyl radicals or superoxide and hydroxyl radicals. Given the position of the band edges and the confinement of the holes, it is likely that the hydroxyl radicals arise from an indirect process such as a Fenton reaction. It is also likely that the superoxide interacts with the holes in a “shuttling” process, preventing its conversion to singlet oxygen.

When conjugated to dopamine, CdSe/ZnS produces significant singlet oxygen. This is likely due to the generated superoxide, formed most probably both in reduction and oxidation reaction processes, namely in the reaction of photogenerated electrons or in the reaction of positively-charged dopamine radicals with oxygen, respectively. As more oxygen is added to the solution, production of singlet oxygen increases.

QD–Dopamine is taken up by dopamine-receptor-bearing PC12 cells. Unconjugated QDs are also endocytosed by these cells, so that a direct comparison of toxicity is possible. The one note of caution seen in our assays was that we often saw large erroneous signals with the green CM-H<sub>2</sub>DCFDA fluorescent ROS reporter dye. This was associated with aggregates of QD–MPA remaining outside the cells, so may represent photo-oxidized QDs that interact directly with the dye. Until this chemistry is worked out, ROS results using this dye will have to be treated with caution.

Cell toxicity corresponded best to levels of singlet oxygen generation. Very little toxicity was seen with QD–MPA, even upon blue-light irradiation for 40 min. However, QD–dopamine led to visible effects on cells, particularly mitochondrial rounding, consistent with previous reports.<sup>25</sup> Effects on cell metabolism were apparent after 30–40 min of blue-light irradiation. The inhibition seen was striking and important, reducing metabolic activity to 20% of baseline. Other nanoparticle–photosensitizer conjugates have reported reduction to 40% of baseline, which is considered sufficient for medical applications such as photodynamic therapy.<sup>18</sup>

The most important implication of this work is that simple biomolecules attached to QDs may ‘photosensitize’ core/shell particles into formation of ROS, which otherwise are not produced by photoexcitation of QDs due to strong exciton

interactions. This leads to cytotoxicity and mitochondrial dysfunction when the particles are taken up into cells, even though release of toxic metals such as Cd<sup>2+</sup> does not occur.<sup>20</sup> It is not likely that this presents any particular environmental danger to complex organisms that may ingest the particles, as the wavelengths of light needed to excite CdSe (UV to blue) have very shallow penetration depths into tissue. However, skin exposure represents a possible hazard, and animal studies will be needed to indicate possible cytotoxic or mutagenic effects on skin. These photosensitized conjugates may also potentially be used as agents for photodynamic therapy (PDT) of superficial cancers such as skin cancer.<sup>26</sup> The hydrophilic nature of the QD conjugates makes them ideal for uptake into inflamed tissues, often a barrier to successful PDT.<sup>27</sup>

## Acknowledgements

This research is funded by US EPA Grant #R833323 and by the National Science and Engineering Research Council of Canada (NSERC) Individual Discovery program. JLN acknowledges salary support from the Canada Research Chairs. The EPR experiments were performed at Argonne under DOE BES Contract No. DE-AC02-06CH11357.

## References

- 1 M. Wainwright, *J. Antimicrob. Chemother.*, 1998, **42**, 13–28.
- 2 E. G. Soltész, S. Kim, R. G. Laurence, A. M. DeGrand, C. P. Parungo, D. M. Dor, L. H. Cohn, M. G. Bawendi, J. V. Frangioni and T. Mihaljevic, *Ann. Thorac. Surg.*, 2005, **79**, 269–277, discussion 269–277.
- 3 A. Hagfeldt and M. Gratzel, *Chem. Rev.*, 1995, **95**, 49–68.
- 4 A. Hagfeldt and M. Gratzel, *Acc. Chem. Res.*, 2000, **33**, 269–277.
- 5 D. Pohle, C. Damm, J. Neuhof, A. Rosch and H. Munstedt, *Polym. Compos.*, 2007, **15**, 357–363.
- 6 C. Sichel, J. Blanco, S. Malato and P. Fernandez-Ibanez, *J. Photochem. Photobiol., A*, 2007, **189**, 239–246.
- 7 B. I. Ipe, M. Lehnig and C. M. Niemeyer, *Small*, 2005, **1**, 706–709.
- 8 D. Y. Lyon, L. Brunet, G. W. Hinkal, M. R. Wiesner and P. J. Alvarez, *Nano Lett.*, 2008, **8**, 1539–1543.
- 9 E. M. Hotze, J. Labille, P. Alvarez and M. R. Wiesner, *Environ. Sci. Technol.*, 2008, **42**, 4175–4180.
- 10 C. Burda, T. C. Green, S. Link and M. A. El-Sayed, *J. Phys. Chem. B*, 1999, **103**, 1783–1788.
- 11 K. Lichtszeld, T. Michalska and I. Kruk, *Z. Phys. Chem.*, 1992, **175**, 117–122.
- 12 A. U. Khan, *Int. J. Quantum Chem.*, 1991, **39**, 251–267.
- 13 A. O. Choi, S. J. Cho, J. Desbarats, J. Lovric and D. Maysinger, *J. Nanobiotechnol.*, 2007, **5**, 1.
- 14 S. Asokan, K. M. Krueger, A. Alkhalwaldeh, A. R. Carreon, Z. Z. Mu, V. L. Colvin, N. V. Mantzaris and M. S. Wong, *Nanotechnology*, 2005, **16**, 2000–2011.
- 15 S. J. Clarke, C. A. Hollmann and F. A. Aldaye, *Bioconjugate Chem.*, 2008, **19**, 562–568.
- 16 C. Flors, M. J. Fryer, J. Waring, B. Reeder, U. Bechtold, P. M. Mullineaux, S. Nonell, M. T. Wilson and N. R. Baker, *J. Exp. Bot.*, 2006, **57**, 1725–1734.
- 17 A. J. Able, D. I. Guest and M. W. Sutherland, *Plant Physiol.*, 1998, **117**, 491–499.
- 18 M. E. Wieder, D. C. Hone, M. J. Cook, M. M. Handsley, J. Gavrilovic and D. A. Russell, *Photochem. Photobiol. Sci.*, 2006, **5**, 727–734.
- 19 T. Pons, H. T. Uyeda, I. L. Medintz and H. Mattoussi, *J. Phys. Chem. B*, 2006, **110**, 20308–20316.
- 20 S. J. Clarke, C. A. Hollmann, Z. Zhang, D. Suffern, S. E. Bradforth, N. M. Dimitrijevic, W. G. Minarik and J. L. Nadeau, *Nat. Mater.*, 2006, **5**, 409–417.
- 21 M. Jiang and J. Zhang, *J. Exp. Bot.*, 2002, **53**, 2401–2410.
- 22 S. Clarke, S. Koshy, J. Zhang, N. Cohen and J. Nadeau, *Z. Phys. Chem.*, 2008, **222**, 851–863.
- 23 www.probes.com.
- 24 W. H. Chan, N. H. Shiao and P. Z. Lu, *Toxicol. Lett.*, 2006, **167**, 191–200.
- 25 S. J. Cho, D. Maysinger, M. Jain, B. Roder, S. Hackbarth and F. M. Winnik, *Langmuir*, 2007, **23**, 1974–1980.
- 26 S. Karrer, R. M. Szeimies, C. Abels and M. Landthaler, *Onkologie*, 1998, **21**, 20–27.
- 27 P. G. Calzavara-Pinton, M. Venturini and R. Sala, *J. Eur. Acad. Dermatol. Venereol.*, 2007, **21**, 293–302.